RSC Advances

PAPER

View Article Online
View Journal | View Issue

Cite this: *RSC Adv.*, 2017, **7**, 15992

In situ growth of TiO_2/SiO_2 nanospheres on glass substrates *via* solution impregnation for antifogging†

Fang Liu,[a] Jie Shen,[b] Wuyi Zhou,[c] Shiying Zhang*[ab] and Long Wan*[a]

Received 24th November 2016
Accepted 9th February 2017

DOI: 10.1039/c6ra27276b

rsc.li/rsc-advances

Uniform TiO_2/SiO_2 nanospheres of 500 nm size were *in situ* fabricated on substrates by a facile soft templating route. The morphologies of the nanospheres on the substrates, as well as the intermediates, were evaluated by FESEM. During the synthesis, a micelle formation process transforming from rod-like micelles to vesicles to lamellar phases was proposed, attributed to the electrostatic self-assembly process of the oppositely charged cationic cetyltrimethyl-ammonium tosylate (CTATos) and anionic Si–OH in the solution. The processed substrates are transparent and super-hydrophilic with good antifogging properties. The homogeneous growth, firm substrate combination, and facile procedures are significantly advantageous for the fabrication method and can be explored with other substrates such as modified electrodes and nanoscale devices for diverse applications.

Introduction

Super-hydrophilic coatings, made of polymers or metal oxides, have great potential for anti-fogging, self-cleaning, anti-fouling, fog-harvesting and so on.[1–9] The super-hydrophilicity can be fabricated either by micro-/nano-scale structure or by high surface concentrations of functional (*e.g.*, hydroxyl) groups.[10–17] Silica is one of the widely used super-hydrophilic materials with superior transparency and anti-fogging performance due to the high surface concentration of hydroxyl groups. Meanwhile, TiO_2 is also widely used for antifogging as the thin sol–gel made polycrystalline films because of its UV-induced super-hydrophilicity.[18] Combining the two metal oxides (SiO_2 and TiO_2), X. Li reported raspberry-like SiO_2–TiO_2 nanoparticle antireflective coatings with superhydrophilicity, high transmittances and good photocatalytic decomposition toward organics.[19] Z. Wu *et al.* reported porous SiO_2/TiO_2 Bragg stacks exhibiting potentially useful superhydrophilicity and self-cleaning properties.[20]

Because of increasing demand of advanced materials with high-tech applications, the development of ceramic nanoparticles has drawn significant attention. Submicron silica particles had been produced and widely used in scientific and industrial applications such as catalysis, electronic, thin film substrate, anti-fogging coating, humidity sensors, and biomedical nanocarriers, because of the controllable size, good monodispersity, favorable biological compatibility, and easy surface modification, as the typical example in advanced ceramic.[21–23] Thus, the synthesis and surface modification of the monodispersed and narrow-sized silica particles have been successfully achieved by the sol–gel method, reverse microemulsion, flame synthesis and so on.[24–26]

Among these methods, the sol–gel process is widely utilized for the preparation of nanocomposites owing to its excellent control of the particle size, monodispersion and well-defined morphology, with the representative of the classical work by Stöber *et al.*[27] Since Grün *et al.* first obtained the submicron MCM-41, the modified Stöber method has been proposed.[28] Based upon a Stöber-like approach, the synthetic compositions can be modified by adding the cationic surfactant into the existing reactants (tetraalkyl silicates, alcohol, water and ammonia) to prepare the uniform mesoporous silica nanoparticles.[29–31] Because the phase of the cationic surfactant can transform among spherical micelles, cylindrical micelles and vesicles in the solution system as the soft template, the silica nanoparticles with various morphologies and mesostructures, such as dual-mesoporous, core–shell and hollow silica nanoparticles have been synthesized.[32–36]

Though the silica nanoparticles can be prepared and applied flexibly, the particle assembly on the substrate is still a real problem. To solve this problem, *in situ* growth method without the follow-up has been used extensively for graphene-like structure, thin films, nanocrystals, metal particles and quantum dots, owing to significant advantages of the interfacial bonding strength.[37–42] However, *in situ* growth of nanospheres on the glass substrates is scarcely reported. Herein, we proposed a facile

[a]College of Materials Science and Engineering, Hunan University, Changsha, 410082, PR China. E-mail: wanlong1799@163.com; cszhangsy@ccsu.edu.cn; Tel: +86-731-84261297

[b]Hunan Key Laboratory of Applied Environmental Photocatalysis, Changsha University, Changsha, 410022, PR China

[c]College of Materials and Energy, South China Agricultural University, Guangzhou, 510642, China

† Electronic supplementary information (ESI) available: Magnification FESEM image, FT-IR spectra, EDS analysis, element distribution (Ti, Si and C) from EDS mapping and TEM image. See DOI: 10.1039/c6ra27276b

strategy to synthesize TiO_2/SiO_2 nanospheres on the glass substrates combining *in situ* growth and the modified Stöber method. The prepared nanospheres with a diameter of ~500 nm were uniformly grown on the substrates, exhibiting a super-hydrophilic property suitable for antifogging.

Experimental

Materials

In this study, all reagents were used directly without further purification. Tetrabutyl orthotitanate (TBOT), tetraethyl orthosilicate (TEOS), acetyl acetone, *n*-butanol, nitric acid, ammonia (28 wt%) and absolute ethyl alcohol were all A.R and provided by Sinopharm Group Co. Ltd, China. The CTATos (cetyltrimethylammonium tosylate) used in the experiment were purchased from Sigma Corporation of America. The glass slides substrates were also obtained from Sinopharm Group Co. Ltd, which should be washed by absolute ethyl alcohol and deionized water alternately three times under ultrasonic processing and then dried in an oven at 80 °C. Deionized water used all over the experiment was self-made in the laboratory.

Synthetic procedures

***In situ* growth of SiO_2 nanoparticles.** The glass substrates were dipped into the mixture of 25 mL TEOS, 3 mL acetyl acetone and 22 mL *n*-butanol for 5 min to assemble the silica source. Then the substrates were transformed into the oven dried to 120 °C for 2 h. After that, the substrates were immersed into a modified Stöber solution containing 1.8 g CTATos, 34.56 g deionized water, 43.2 g absolute ethanol and 11.52 mL ammonia (28 wt%) for 6 h, 12 h, 24 h and 48 h respectively to *in situ* form the siloxane particles on the substrates. After dried at 120 °C in the oven, the samples were finally heated at 500 °C for 2 h to obtain the *in situ* growing SiO_2 on the substrates. Based on the immersing time, the samples were named as SP_6, SP_{12}, SP_{24} and SP_{48} respectively.

Preparation of TiO_2/SiO_2 nanospheres on the substrate. The TiO_2/SiO_2 nanospheres were prepared by coating titanium gel on the 48 h immersed substrate (*in situ* with un-heating SP_{48}) and then heated once for 2 h at 500 °C. The titanium gel was prepared *via* the typical sol–gel method involving 8.00 g TBOT, 1.21 g acetyl acetone, 65 g *n*-butanol, 0.3 mL nitric acid and 0.4 g deionized water. The siloxane spheres were *in situ* formed premeditatedly on the substrates as the above steps by 48 h immersing. After dried at 120 °C in the oven, the titanium gel was then dip-coated on the substrates. With a re-drying process, the uniform TiO_2/SiO_2 nanospheres were finally synthesized on the substrate after heating at 500 °C for 2 h.

Characterization

The morphologies of the *in situ* growing particles on the substrate were evaluated by field emission scanning electron microscopy (FESEM, JSM-6700F, SHIMADZU). The composition of the TiO_2/SiO_2 nanospheres was detected by the Energy Dispersive Spectrometer (EDS). Finally, the contact angles of the membranes were measured by a JC2000D2 Tensiometer and Contact Angle Meter.

Results and discussion

The morphologies of the *in situ* growth samples were examined by FESEM, as shown in Fig. 1. The images displayed that the blank substrate was flat and smooth, the simple TEOS assembling making no much change, seen in Fig. 1a and b. As displayed in Fig. 1c, the spherical siloxane particles *in situ* grew on the TEOS assembled substrate after 48 h immersing in the modified Stöber solution. As the red arrows indicated, most of the siloxane spheres were imperfect and appeared the hollow structure, due to the syneresis of the templates. In view of this, we perceived that the cationic surfactant CTATos might form a vesicles phase in the solution as the soft template for the hollow cavity.[43,44] With coated by the prepared titanium gel, as shown in Fig. 1d, the spherical siloxane particles were filled and encapsulated to be the complete spheres. After a heat treatment of 500 °C, the structure of the TiO_2/SiO_2 nanospheres were still complete kept as exhibited in Fig. 1f, whereas the fragile spherical silica particles were collapsed to be small protuberances without the titanium coating, shown in Fig. 1e. The size shrinkage of the TiO_2/SiO_2 nanospheres can be attributed to the thermal condensation of silica and titanium.

To show the homogeneous growth of the TiO_2/SiO_2 nanospheres on the substrate, the macrograph of FESEM was provided in Fig. 2a. The elemental analysis was also tested by EDS (Fig. 2b) and the alveolate inner cavity of the nanospheres was shown in the inset graph. From the EDS graph, the peaks of Si, O and Ti introduced by the experiment were observed. The other elements like Na, Mg, Al and Ca could be attributed to the composition of the glass substrate. The element Pt was attributed to the metal spraying before the FESEM test.

The EDS analysis of the unheated TiO_2/SiO_2 nanospheres has been provided in the ESI file as Fig. S1,† from which the distinct peak of C was observed. Considering of the almost invisible peak of C in the heated sample (Fig. 2b), it can be perceived that the carbon in the system was almost completely removed. What's more, the element distribution (Ti, Si and C) from EDS mapping of the TiO_2/SiO_2 nanospheres before and after the calcination treatment has been provided in the ESI file as Fig. S2.† As shown in Fig. S2,† the carbon element concentrated in the cavity of the nanospheres before the calcination and

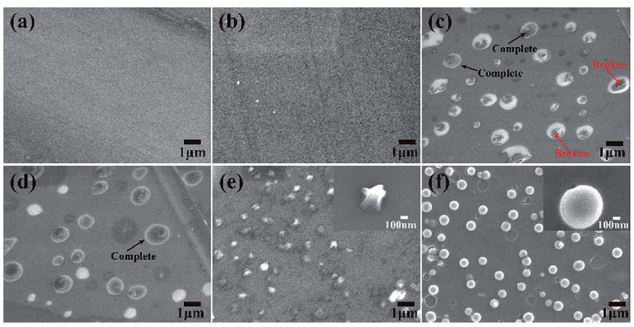

Fig. 1 FESEM images of blank glass substrate (a), TEOS assembled substrate (b), the un-heating SP_{48} (c), the un-heating TiO_2/SiO_2 nanospheres (d), the sample SP_{48} (e) and the TiO_2/SiO_2 nanospheres (f) grown *in situ* on the glass substrate.

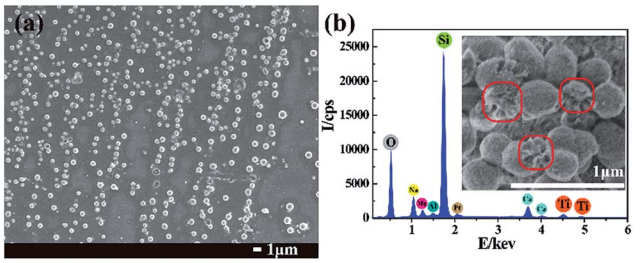

Fig. 2 The macrograph (a), the EDS analysis (b) and the broken cavity (inset) of the TiO_2/SiO_2 nanospheres.

disappeared after the heat treatment. The result proved the spherical multilamellar vesicle template structure forming the lamellar phases in the immersing solution and the complete removal of the template after the calcination treatment.

To further investigate the *in situ* growing mechanism of the silica particles in the immersing solution, the SiO_2 samples with different immersing time were observed using FESEM and the results were shown in Fig. 3. The *in situ* growing processes of the silica particles in the immersing solution were exhibited explicitly in Fig. 3a–d. At the initial 6 h, the scattered silica particles dispersed on the substrate and some of them assembled the rod-like nicks. Going through another 6 h, the silica particles assembled as several circular holes which seemed like the surface was engraved by spherical templates. After 24 h immersing, the silica particles tended to grow upwards from the edge of the circle and finally formed a bowl-like structure. After immersed for 48 h, the particles grew to the complete spherical structure, combining with Fig. 1c, and collapsed to be protuberances with heat treatment. In addition, the average size of rod-like silica particles is at the length of about 125 nm and diameter of 15 nm from the heated sample SP_6 (as seen in Fig. S3†). The size of the circular holes is about 500 nm from the heated sample SP_{12} (Fig. 3b). The size of the bowl-like structure is about 300 nm from the heated sample SP_{24} (Fig. 3c). The size of the spherical structure is about 800 nm from the un-heating SP_{48} (Fig. 1c).

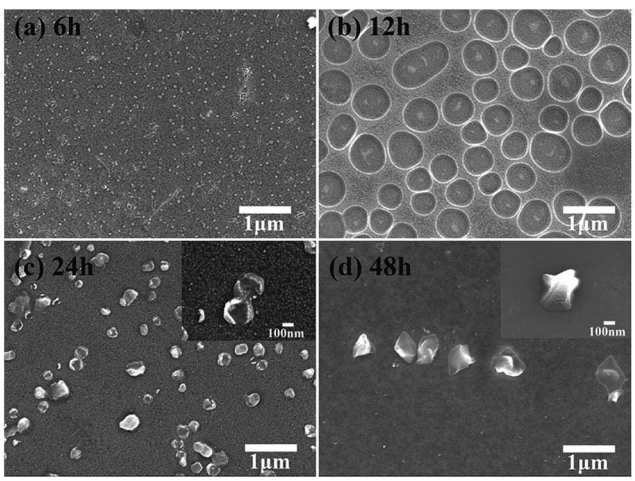

Fig. 3 FESEM images of the *in situ* growing SiO_2 particles with different immersing time. Based on the immersing time, the images of SP_6 (a), SP_{12} (b), SP_{24} (c) and SP_{48} (d) were shown respectively.

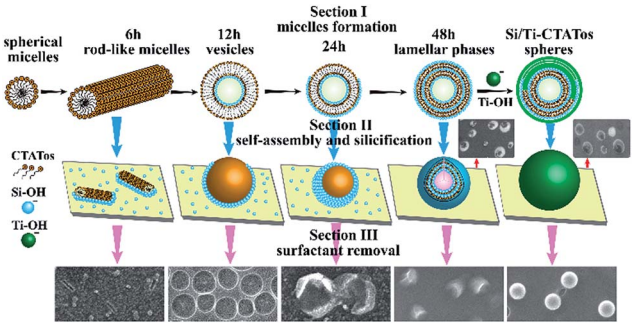

Fig. 4 The *in situ* synthesis mechanism of TiO_2/SiO_2 nanospheres.

Based on the incremental immersing FESEM images, the *in situ* synthesis mechanism of the TiO_2/SiO_2 nanospheres was investigated in Fig. 4. Due to the perceived point, the gradual micelle formation was the critical step in the synthesis. Inspired by the work of L. Han *et al.*,[45] the single-tailed anionic surfactants and the cationic silane producing lamellar phases to prepare the silica nanospheres with diameter of 300 nm, the oppositely charged cationic CTATos and anionic Si–OH might also form the vesicles and lamellar phases in this experiment. At the initial 6 h, the cationic CTATos was used as the template and several rod-like micelles were formed in the immersing solution.[46] With the gradually hydrolyzing of the adhering silane, the increased anionic Si–OH combined CTATos to form the vesicles at 12 h.[47] As time passed, the Si–OH aggregated and condensed along the cationic vesicles, finally forming the lamellar phases by layer-by-layer electrostatic self-assembly of Si–OH and CTATos in the immersing solution and depositing on the substrate surface.[48] The hydrolyzed silane further condensed around the lamellar micelles, and produced the hollow spherical organic silica structures on the substrate after immersing for 48 h.[49] As the concentration of Si–OH decreased with distance from the substrate, lots of spherical silica structures were incomplete, and the vulnerable silica layers collapsed easily after heat treatment. The titanium gel was coated before heat-treatment to keep the complete spherical structures, and the gel might fill the hollow cavity partly (shown in the inset of Fig. 2b) because of the high solubility of CTATos in gel solution.

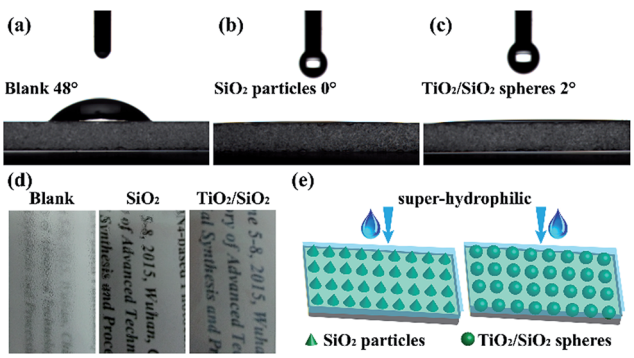

Fig. 5 Contact angle of the blank substrate (a), substrate with SiO_2 particles (b) and substrate with TiO_2/SiO_2 nanospheres (c); the anti-fogging property of the samples (d); the wetting schematic diagram of the *in situ* synthesis samples (e).

The wettability of the processed substrates was detected *via* the contact angle test. As shown in Fig. 5a–c, the unprocessed substrate possessed a contact angle (CA) of 48°, whereas a good super-hydrophilicity was exhibited after the *in situ* modification (CA < 5°). Benefiting from the super-hydrophilicity, the processed substrates exhibited good antifogging properties, as shown in Fig. 5d. The *in situ* synthesized SiO_2 particles and TiO_2/SiO_2 nanospheres distributed on the substrates to form a rough topography as shown in Fig. 5e. In addition with the hydrophilic chemical composition, the super-hydrophilic surface was finally prepared.[50]

Conclusions

In this study, we have developed a facile soft templating route for *in situ* fabrication of TiO_2/SiO_2 nanospheres on the glass substrates. During the solution impregnation in synthesis, a micelles formation process transforming from rod-like micelles to vesicles to lamellar phases was assumed based on the incremental immersing FESEM images. The micelles formation mechanism was investigated as the unique layer-by-layer electrostatic self-assembly process of the oppositely charged cationic CTATos and anionic Si–OHs in the solution. The hydrolyzed silane finally condensed around the lamellar micelles, affording spherical structures. The prepared TiO_2/SiO_2 nanospheres had a uniform dimension of ~500 nm. The homogeneous growth and firm substrate combination provides significant advantage for *in situ* fabrication compared to traditional nanopowder coatings. The processed substrates are transparent and super-hydrophilic, possessing good antifogging property. As the *in situ* fabrication can be achieved *via* simple modified Stöber solution impregnation at room temperature, the synthetic method can be easily explored to other substrates such as modified electrode and nano-scale devices, for diverse applications.

Acknowledgements

We are grateful for the financial support from the National Natural Science Foundation of China (51272032), the Hunan Provincial Natural Science Foundation of China (14JJ5010), the Graduate Student Research Innovation Project in Hunan Province (No. 022900/521293321) and the Aid Program for Science and Technology Innovative Research Team in Higher Educational Institutions of Hunan Province.

Notes and references

1 X. Tang, T. Wang, F. Yu, X. Zhang, Q. Zhu, L. Pang, G. Zhang and M. Pei, *RSC Adv.*, 2013, **3**, 25670–25673.
2 Q. Mao, D. Zeng, K. Xu and C. Xie, *RSC Adv.*, 2014, **4**, 58101–58107.
3 I. You, Y. C. Seo and H. Lee, *RSC Adv.*, 2014, **4**, 10330–10333.
4 S. Nishimoto and B. Bhushan, *RSC Adv.*, 2012, **3**, 671–690.
5 D. Tahk, T. Kim, H. Yoon, M. Choi, K. Shin and K. Y. Suh, *Langmuir*, 2010, **26**, 2240–2243.
6 P. Patel, K. C. Chang and D. D. Meng, *JALA*, 2010, **15**, 114–119.
7 R. P. Garrod, L. G. Harris, W. C. Schofield, J. Mcgettrick, L. J. Ward, D. O. Teare and J. P. Badyal, *Langmuir*, 2007, **23**, 689–693.
8 M. L. Carman, T. G. Estes, A. W. Feinberg, J. F. Schumacher, W. Wilkerson, L. H. Wilson, M. E. Callow, J. A. Callow and A. B. Brennan, *Biofouling*, 2006, **22**, 11–21.
9 R. Blossey, *Nat. Mater.*, 2003, **2**, 301–306.
10 F. Dai, M. Zhang, B. Hu, Y. Sun, Q. Tang, M. Du and X. Zhang, *RSC Adv.*, 2015, **5**, 3574–3580.
11 J. Liu, F. Chen, H. Zheng, S. Liu, J. Sun, S. Huang, J. Song, Z. Jin and X. Liu, *RSC Adv.*, 2016, **6**, 79437–79447.
12 T. Li, J. Shen, Z. Zhang, S. Wang and D. Wei, *RSC Adv.*, 2016, **6**, 40656–40663.
13 V. A. Ganesh, A. S. Nair, H. K. Raut, T. M. Walsh and S. Ramakrishna, *RSC Adv.*, 2011, **2**, 2067–2072.
14 J. Zhao, A. Meyer, L. Ma, X. Wang and W. Ming, *RSC Adv.*, 2015, **5**, 102560–102566.
15 W. Zhang, L. Zhu, W. Li, H. Ye and H. Liu, *RSC Adv.*, 2016, **6**, 92252–92258.
16 H. Xu, L. Liu, F. Wu, D. Xu and N. Lu, *RSC Adv.*, 2015, **5**, 28014–28018.
17 B. Dudem, J. W. Leem and J. S. Yu, *RSC Adv.*, 2015, **6**, 3764–3773.
18 W. Y. Wong, N. Nasiri, A. Rodriguez, D. Nisbet and A. Tricoli, *J. Mater. Chem. A*, 2014, **2**, 15575–15581.
19 X. Li and J. He, *ACS Appl. Mater. Interfaces*, 2013, **5**, 5282–5290.
20 Z. Wu, L. Daeyeon, R. Michael and C. Robert, *Small*, 2007, **3**, 1445–1451.
21 I. A. Rahman and V. Padavettan, *J. Nanomater.*, 2012, **2012**, 2817–2827.
22 Z. Li, J. C. Barnes, A. Bosoy, J. F. Stoddart and J. I. Zink, *Chem. Soc. Rev.*, 2012, **41**, 2590–2605.
23 F. C. Cebeci, Z. Wu, L. Zhai, R. E. Cohen and M. F. Rubner, *Langmuir*, 2006, **22**, 2856–2862.
24 Q. H. Zeng, D. Z. Wang, A. B. Yu and G. Q. Lu, *Nanotechnology*, 2002, **13**, 549–553.
25 T. T. Y. Tan, S. Liu, Y. Zhang, M. Y. Han and S. T. Selvan, *Comprehensive Nanoscience & Technology*, 2011, vol. 5, pp. 399–441.
26 E. Reverchon and R. Adami, *J. Supercrit. Fluids*, 2006, **37**, 1–22.
27 W. Stöber, A. Fink and E. Bohn, *J. Colloid Interface Sci.*, 1968, **26**, 62–69.
28 M. Grün, I. Lauer and K. K. Unger, *Adv. Mater.*, 1997, **9**, 254–257.
29 Y. Lin, C. Tsai, H. Huang, C. Kuo, Y. Hung, D. Huang, A. Yaochang Chen and C. Mou, *Chem. Mater.*, 2005, **17**, 1–6.
30 K. Yano and Y. Fukushima, *J. Mater. Chem.*, 2004, **14**, 1579–1584.
31 T. Nakamura, M. Mizutani, H. Nozaki, N. Suzuki and K. Yano, *J. Phys. Chem. C*, 2007, **165**, 1093–1100.
32 Y. Q. Yeh, B. C. Chen, H. P. Lin and C. Y. Tang, *Langmuir*, 2006, **22**, 6–9.
33 T. Suteewong, H. Sai, R. Cohen, S. Wang, M. Bradbury, B. Baird, S. M. Gruner and U. Wiesner, *J. Am. Chem. Soc.*, 2011, **133**, 172–175.

34 J. Liu, Q. Yang, L. Zhang, H. Yang, J. Gao and C. Li, *Chem. Mater.*, 2008, **20**, 4268–4275.
35 J. Liu, S. Z. Qiao, S. Budi Hartono and G. Q. Lu, *Angew. Chem., Int. Ed.*, 2010, **49**, 4981–4985.
36 T. W. Kim, P. W. Chung and S. Y. Lin, *Chem. Mater.*, 2010, **22**, 5093–5104.
37 G. Xi, J. Ye, Q. Ma, N. Su, H. Bai and C. Wang, *J. Am. Chem. Soc.*, 2012, **134**, 6508–6511.
38 Z. Teng, G. Zheng, Y. Dou, W. Li, C. Y. Mou, X. Zhang, A. M. Asiri and D. Zhao, *Angew. Chem., Int. Ed.*, 2012, **51**, 2173–2177.
39 F. Liu, L. Yi, K. Zhang, W. Bo, Y. Chang, Y. Lai, Z. Zhang, L. Jie and Y. Liu, *Sol. Energy Mater. Sol. Cells*, 2010, **94**, 2431–2434.
40 H. Lee, S. W. Yoon, E. J. Kim and J. Park, *Nano Lett.*, 2007, **7**, 778–784.
41 F. Gong, H. Wang, X. Xu, G. Zhou and Z. S. Wang, *J. Am. Chem. Soc.*, 2012, **134**, 10953–10958.
42 H. Chang, X. Lv, H. Zhang and J. Li, *Electrochem. Commun.*, 2010, **12**, 483–487.
43 H. Yin, Z. Zhou, J. Huang, R. Zheng and Y. Zhang, *Angew. Chem., Int. Ed.*, 2003, **42**, 2188–2191.
44 L. Pan, Q. He, J. Liu, Y. Chen, M. Ma, L. Zhang and J. Shi, *J. Am. Chem. Soc.*, 2012, **134**, 5722–5725.
45 L. Han, C. Gao, X. Wu, Q. Chen, P. Shu, Z. Ding and S. Che, *Solid State Sci.*, 2011, **13**, 721–728.
46 K. Zhang, L. L. Xu, J. G. Jiang, N. Calin, K. F. Lam, S. J. Zhang, H. H. Wu, G. D. Wu, B. Albela and L. Bonneviot, *J. Am. Chem. Soc.*, 2013, **135**, 2427–2430.
47 P. Kipkemboi, A. Fogden, A. Viveka Alfredsson and K. Flodström, *Langmuir*, 2001, **17**, 5398–5402.
48 H. P. Hentze, S. R. Raghavan, M. Kelvey and E. W. Kaler, *Langmuir*, 2003, **19**, 1069–1074.
49 J. Liu, S. B. Hartono, Y. G. Jin, Z. Li, G. Q. Lu and S. Z. Qiao, *J. Mater. Chem.*, 2010, **20**, 4595–4601.
50 B. Su, Y. Tian and L. Jiang, *J. Am. Chem. Soc.*, 2015, **138**, 1727–1748.